The periciliary ring in polarized epithelial cells is a hot spot for delivery of the apical protein gp135

Emily H. Stoops,[1,2] Michael Hull,[1,2] Christina Olesen,[1,2] Kavita Mistry,[1,2] Jennifer L. Harder,[3] Felix Rivera-Molina,[1] Derek Toomre,[1] and Michael J. Caplan[1,2]

[1]Department of Cell Biology and [2]Department of Cellular and Molecular Physiology, Yale University School of Medicine, New Haven, CT 06520
[3]Department of Internal Medicine, University of Michigan Medical School, Ann Arbor, MI 48109

In polarized epithelial cells, newly synthesized cell surface proteins travel in carrier vesicles from the trans Golgi network to the apical or basolateral plasma membrane. Despite extensive research on polarized trafficking, the sites of protein delivery are not fully characterized. Here we use the SNAP tag system to examine the site of delivery of the apical glycoprotein gp135. We show that a cohort of gp135 is delivered to a ring surrounding the base of the primary cilium, followed by microtubule-dependent radial movement away from the cilium. Delivery to the periciliary ring was specific to newly synthesized and not recycling protein. A subset of this newly delivered protein traverses the basolateral membrane en route to the apical membrane. Crumbs3a, another apical protein, was not delivered to the periciliary region, instead making its initial apical appearance in a pattern that resembled its steady-state distribution. Our results demonstrate a surprising "hot spot" for gp135 protein delivery at the base of the primary cilium and suggest the existence of a novel microtubule-based directed movement of a subset of apical surface proteins.

Introduction

The plasma membranes of polarized epithelial cells are characterized by the presence of distinct apical and basolateral membrane domains, each composed of different subsets of lipids and membrane proteins. To generate and maintain this polarity, membrane proteins bound for each membrane are sorted into separate carrier vesicles and their trafficking is tightly regulated (Ellis et al., 2006; Cao et al., 2009; Stoops and Caplan, 2014). The asymmetrical distribution of proteins in these cells is essential for epithelial tissues to perform their physiological functions, including the vectorial transport of solutes against steep concentration gradients.

Numerous studies have explored the trafficking pathways pursued by various apical and basolateral proteins and have investigated the properties of the carrier vesicles that mediate this transport (Stoops and Caplan, 2014). Despite this growing body of work and the physiological importance of polarized trafficking, relatively little is known about the sites at which carrier vesicles fuse with target membrane domains. Previous studies have suggested that tight junctions may serve as a "hot spot" for vesicle delivery. Tight junctions form a functional barrier between the apical and basolateral membranes. The apical membrane protein aminopeptidase reappears at the apical surface in close proximity to tight junctions (Louvard, 1980) after its endocytosis and recycling. Similarly, some basolateral proteins appear to be delivered to the lateral surface immediately below the junctions in a region where components of the exocyst are concentrated (Kreitzer et al., 2003). More recently, vesicles containing rhodopsin-GFP were observed to fuse at sites distributed randomly throughout the apical membrane (Thuenauer et al., 2014).

The route taken by newly synthesized apical proteins before their surface delivery is also the subject of debate. Several glycophosphatidylinositol (GPI)-anchored protein constructs expressed in polarized renal cells in culture were shown to appear first at the basolateral surface, followed by transcytosis to the apical membrane (Polishchuk et al., 2004). Subsequent work, however, has suggested that these proteins pursue a direct route from the Golgi complex to the apical plasma membrane (Paladino et al., 2006).

Here, we use the powerful SNAP tag labeling technique to determine whether the apical glycoprotein gp135 is delivered to hot spots within the apical membrane. gp135, also known as podocalyxin, is critically important in maintaining glomerular filtration and podocyte structure in the renal glomerulus (Kerjaschki et al., 1984; Doyonnas et al., 2001) and is involved in apical membrane formation in MDCK cells (Meder et al., 2005). By taking advantage of a SNAP tag appended to the extracellular domain of gp135, we were able to separately label the preexisting pool of gp135 protein at the cell surface and the

Mr. Hull died on 10 July 2015.

Correspondence to Michael J. Caplan: michael.caplan@yale.edu

Abbreviations used in this paper: BG, O^6-benzylguanine; CHX, cycloheximide; GPI, glycophosphatidylinositol; MDCK-S, MDCK cells stably transfected with SNAP-tagged gp135; PEG, polyethylene glycol; PLAP, placental alkaline phosphatase; SNAP-Block, SNAP Surface Block.

The Rockefeller University Press $30.00
J. Cell Biol. Vol. 211 No. 2 287–294
www.jcb.org/cgi/doi/10.1083/jcb.201502045

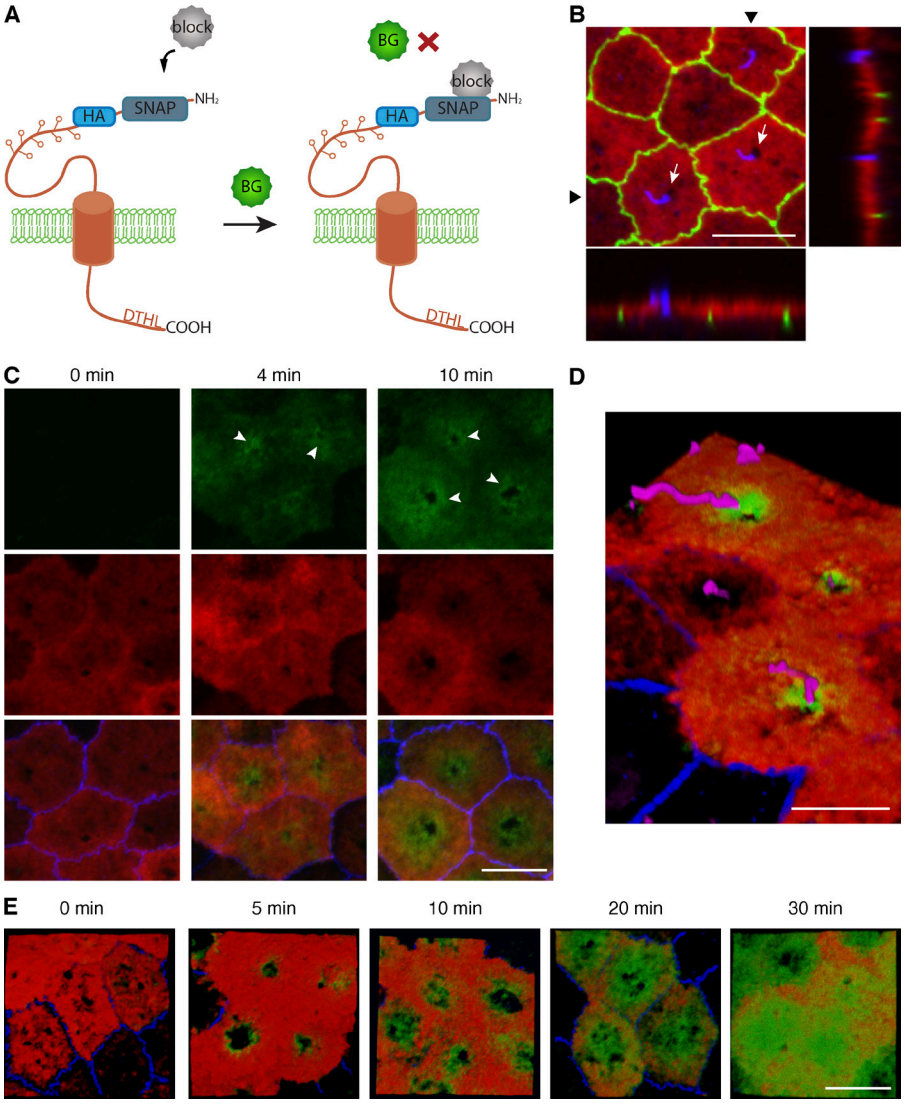

Figure 1. **SNAP-tagged gp135 traffics to the apical membrane and is delivered to the periciliary ring.** (A) Schematic view of the SNAP-tagged gp135 construct and BG labeling. DTHL is the amino acid sequence of the C termins of the gp135 protein. (B) MDCK cells stably expressing SNAP-gp135 were fixed, stained with BG549 (red), and processed for immunofluorescence (ZO1, green; acetylated tubulin, blue). Arrowheads indicate positions of the orthogonal views. Arrows indicate ciliary exclusion zones. (C–E) Old surface SNAP-gp135 was labeled to saturation with BG549 (red). Newly delivered SNAP-gp135 was labeled with BG488 (green) after the indicated times at 37°C (ZO1, blue). Arrowheads indicate periciliary rings. (D and E) 3D reconstructions demonstrating SNAP-gp135 periciliary delivery. (D) Time = 8 min (acetylated tubulin, magenta). Bars, 10 µm.

pool of gp135 protein delivered to the apical membrane during a specified time period. We show here that newly synthesized gp135 is delivered to a ring at the base of the primary cilium. Furthermore, the cell surface pool of gp135 protein underwent a microtubule-dependent directed radial motion toward the periphery of the apical membrane. We also demonstrate that a portion of the pool of gp135 traffics through the basolateral membrane before its apical membrane insertion. These results define a new hot spot for the biosynthetic delivery of an apical protein and provide new insight into the trafficking pathways used in polarized cells.

Results and discussion

To study the trafficking of gp135, we generated a version of this protein in which a SNAP tag and an HA epitope tag were inserted into its extracellular N-terminus immediately distal to its signal sequence (Fig. 1 A). The SNAP tag, a modified form of the enzyme O^6-alkylguanine-DNA alkyltransferase, allows temporally and spatially defined cohorts of proteins to be selectively labeled and detected (Juillerat et al., 2003; Keppler et al., 2004). The tag binds covalently to O^6-benzylguanine (BG), resulting in the irreversible transfer of the substituted benzyl group to the reactive thiol within the SNAP tag. BG derivatives bearing fluorophores, biotin, or other groups can be used to label a SNAP-tagged protein (Farr et al., 2009; Maurel et al., 2010; Sun et al., 2011; Lukinavičius et al., 2013).

MDCK cells stably transfected with SNAP-tagged gp135 (MDCK-S cells) can be labeled with 2xDyomics549-conjugated BG (BG549) to yield a robust signal (Fig. 1 B). The SNAP tag renders the fusion protein unrecognizable by a commonly used antibody directed against gp135 by both Western blot (Fig. S1 A) and immunofluorescence (not depicted), making it difficult to determine precisely the expression levels of the fusion protein versus native gp135. It is worth noting, however, that compared with untransfected cells, we detect 17.55% ± 2.27% ($P < 0.05$) as much gp135 with anti-gp135 in MDCK-S cells, suggesting that expression of the tagged form reduces the expression or accumulation of the endogenous protein. At steady state in MDCK-S cells, SNAP-tagged gp135 (SNAP-gp135) localizes primarily to the apical membrane but is not present in the primary cilium or in the area surrounding its base (Fig. 1 B). This localization is consistent with that of endogenous gp135 (Francis et al., 2011), suggesting that the SNAP tag does not perturb the protein's trafficking or localization. The gp135-excluding

subdomain of the apical membrane has previously been defined as the ciliary membrane domain (Francis et al., 2011). Because in the context of the present study this domain is defined by what is excluded from it, presumably by virtue of the properties of the septin diffusion barrier (Hu et al., 2010) or of a condensed lipid environment at the ciliary base (Vieira et al., 2006), we elected to refer to this region as the ciliary exclusion zone.

Using a pulse-chase labeling strategy with multiple BG substrates, we separately and specifically labeled both "old" and newly delivered gp135 to examine the location of gp135 delivery within the apical membrane. The pool of old SNAP-gp135 present at the apical surfaces of MDCK-S cells at the start of the experiment was labeled with cell-impermeable BG549. To ensure saturation of the labeling capacity of the preexisting apical pool of SNAP-gp135, a subsequent incubation with a nonfluorescent, cell-impermeable BG derivative (SNAP-Surface Block [SBG-Block]) was performed. Labeling of the old pool of gp135 was performed at 4°C to prevent protein trafficking. Importantly, incubation of cells at 4°C did not affect the extent of staining for ciliary microtubules (Fig. S1, B and C). After labeling of old SNAP-gp135, cells were incubated at the trafficking-permissive temperature of 37°C for 0–30 min. Newly delivered protein was then labeled with membrane-impermeable BG488 at 4°C. As a control to assess the saturation of old protein with BG549 and SBG-Block, cells were labeled with BG488 immediately after labeling with SBG-Block (Fig. 1 C, 0 min). The observed lack of BG488 signal in this control demonstrates that any protein labeling with this fluorophore at later time points is attributable to newly delivered protein.

After 4–10 min of incubation at 37°C, BG488-labeled ("new") gp135 was present at highest intensity in a ring surrounding the base of the cilium (Fig. 1, C and D). Cilia were visualized by labeling with an antibody directed against acetylated tubulin (Fig. 1, B [blue] and D [magenta]). This pattern was not an artifact of the domed shape of the apical membrane because it was not observed with old gp135 and was observed in maximum intensity projections (Fig. 2 A and Video 1) and 3D reconstructions of confocal stack images (Fig. 1, D and E). With increasing time at 37°C, the intensity of newly delivered gp135 in the peripheral regions of the apical membrane increased. By 20 min, the new gp135 uniformly covered the somatic apical membrane (not including the ciliary exclusion zone). Old SNAP-gp135 was observed to be internalized within 10 min after incubation at 37°C (Fig. S1 D). These structures, which presumably represent endosomes, were rarely detected under the periciliary region. Instead, they were found predominantly toward the periphery of a central zone of low gp135 intensity.

The experiments described in the preceding paragraphs detect newly delivered gp135 without distinguishing between newly synthesized protein and protein that has been recycled to the apical membrane after being internalized from the cell surface before the BG549 labeling step. To determine whether both pools are delivered to the periciliary ring, we observed the delivery of each pool separately. To track recycling protein, the delivery assay was performed after cycloheximide (CHX) treatment to inhibit protein synthesis. In the absence of new protein synthesis, only recycling protein will be delivered to the apical membrane and available for BG488 binding. Newly delivered recycling protein was observed over the entire apical membrane after 5 min, and no enhanced periciliary ring staining was observed under these conditions (Fig. 2 A).

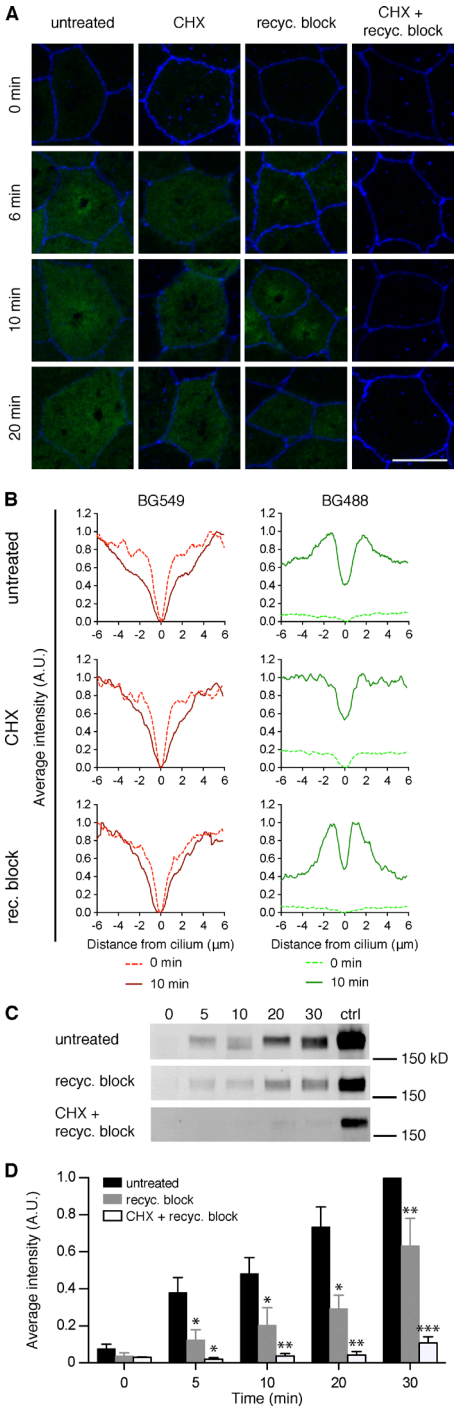

Figure 2. **Newly synthesized, not recycling, gp135 is delivered to the periciliary ring.** (A and B) Newly delivered gp135 (green) in cells treated with CHX and/or with an extended recycling block with BG549. (A) Maximum-intensity projections of z-stacks representative of three independent experiments (ZO1, blue). Bar, 10 µm. (B) Mean line intensity of BG549 (old) and BG488 (newly delivered) across the apical membrane (0 min, dashed line; 10 min, solid line). At 10 min, untreated and recycling block-treated, but not CHX-treated, samples display peaks of heightened BG488 intensity proximal to the cilium. n = 15 cells/condition. 0-min BG488 values were normalized to the highest mean value of BG488 at 10 min for each condition. (C) Newly delivered, SNAP782-labeled gp135 was detected by Licor after SDS-PAGE. Control samples were not blocked before SNAP782 labeling. (D) Quantification of C normalized to SNAP782 intensity in untreated cells at 30 min. Values represent mean ± SEM of three (recycling block, gray; double block, white) or six (untreated, black) independent experiments. *, $P < 0.05$; **, $P < 0.001$; ***, $P < 0.0001$.

For the reciprocal experiment, we performed an extended incubation with BG549 for 2 h at 37°C. Performing the incubation with the fluorophore-conjugated BG for a longer period at a trafficking-permissive temperature ensures that the pool of recycling gp135 that exchanges between the cell surface and endosomal compartments is fully labeled with BG549. This effectively blocks the recycling protein pool and eliminates its availability for subsequent labeling steps, meaning only that pool of newly delivered SNAP-gp135 that is newly synthesized will be available to be labeled with BG488. Hence, we refer to the extended BG549 incubation as a recycling block. Newly delivered SNAP-gp135 was detected at the apical membrane after 5 min at 37°C. The periciliary ring labeling pattern was even more prominent in cells subjected to the recycling block than in untreated cells, whereas the intensity of the BG488 signal in the outer regions of the apical membrane was decreased (Fig. 2 A). Quantification of mean BG488 line intensity values (Fig. 2 B, green) further demonstrates the differential pattern of delivery of newly synthesized and recycling gp135. In untreated cells after 10 min at 37°C (solid green line), the highest concentrations of newly delivered SNAP-gp135 were proximal to the ciliary exclusion zone, as represented by peaks on either side of the cilium. The periciliary peaks in BG488 intensity were abolished in CHX-treated cells and enhanced after an extended BG549 block to prevent labeling of recycling protein. Our data strongly suggest that newly synthesized gp135, but not recycling gp135, is delivered to the periciliary ring.

As a control, cells were treated with both CHX and an extended recycling block. Under these double block conditions, no BG488 signal was observed at any time point, demonstrating efficient block of both the newly synthesized and recycling pools (Fig. 2 A). Similar results were achieved using biochemical methods to detect newly delivered surface SNAP-gp135. For these experiments, recycling block conditions were used to block old protein as before, but newly delivered protein was labeled with cell-impermeable SNAP782, an infrared fluorophore-conjugated BG reagent. SNAP782-bound gp135 in cell lysates was detected on a LI-COR Odyssey scanner after SDS-PAGE (Fig. 2 C). The newly synthesized pool represents roughly half of the population of SNAP-gp135 that is delivered to the cell surface during a 30-min incubation (Fig. 2 D). Consistent with what was observed by confocal microscopy, a double block nearly abolishes biochemical detection of newly delivered protein.

These experiments also revealed a surprising trend in the localization of old SNAP-gp135 at the apical membrane (Fig. 2 B). At 0 min, old gp135 was present throughout the apical membrane, excluding the ciliary exclusion zone. At later time points, a central region exhibiting low-intensity old gp135 signal progressively increased in size. The signal corresponding to the old BG549-labeled SNAP-gp135 was more prominent toward the cell periphery (Fig. 3 C). This zone of central clearing was also observed by live imaging of MDCK-S cells after labeling with BG488 (Video 2). Interestingly, the zone of central clearing did not progress all the way to the tight junctions and instead was limited to a circle ∼4–5 µm in diameter. The directed nature of this movement away from the periciliary zone suggested that it was mediated by a mechanism other than simple diffusion.

We next sought to determine whether the periciliary delivery and central clearing that were detected with SNAP-gp135 are general phenomena observed with other apical proteins.

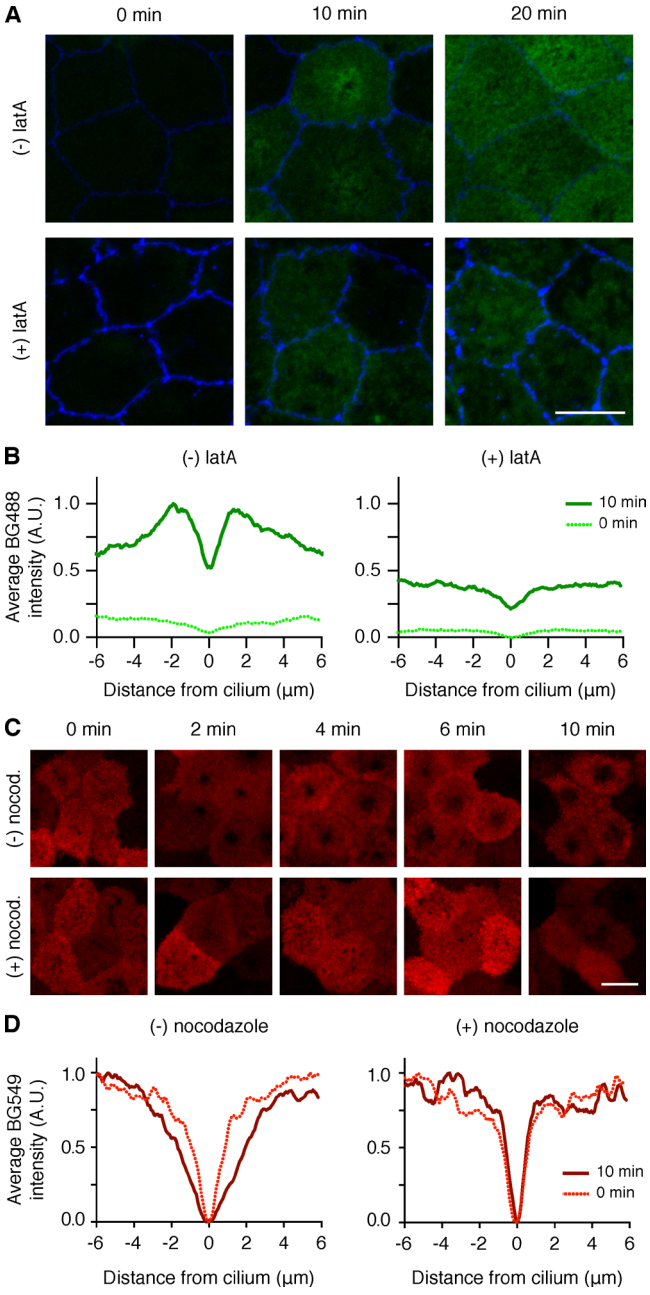

Figure 3. **Periciliary delivery is actin dependent and old gp135 is cleared from the periciliary region in a microtubule-dependent manner.** (A) Newly delivered gp135 (BG488, green) after 0–20 min at 37°C in untreated or latrunculin A (latA)-treated MDCK-S cells (ZO1, blue). (B) Mean line scan intensity of newly delivered gp135, as in Fig. 2 B, demonstrates inhibition of periciliary delivery in latA-treated cells. All values were normalized to highest mean value of BG488 intensity at 10 min in untreated cells. (C) Old surface gp135 (BG549) after 0–10 min at 37°C in untreated or nocodazole-treated MDCK-S cells. (D) Mean line scan intensity of old gp135, as in Fig. 2 B, demonstrates inhibition of gp135 clearing from the periciliary region in nocodazole-treated cells. (B and D) 0 min, dashed line; 10 min, solid line. n = 15 cells per condition. For both experiments, data are representative of three independent experiments. Bars, 10 µm.

To examine surface delivery of another apical protein, we used a previously characterized MDCK cell line expressing SNAP-tagged Crumbs3a (Harder et al., 2012). Like the native Crumbs3a protein, SNAP-Crumbs3a is distributed over the entire apical surface and is more highly concentrated at or near the

tight junctions (Harder et al., 2012; Fig. S2 A). Using a protocol similar to that employed in Fig. 1, we followed the initial delivery of intracellular SNAP-Crumbs3a to the cell surface after a block of the old surface-exposed pool. We found that SNAP-Crumbs3a is delivered to the apical membrane in a pattern that closely resembles its steady-state distribution (Fig. S2 B). We never observed delivery of Crumbs3a to the periciliary region. Crumbs3a forms stable attachments with a submembranous anchoring complex that includes the proteins PALS and PATJ (Makarova et al., 2003), and transmembrane gp135 has been shown to interact directly with cytoskeletal components (Ojakian and Schwimmer, 1988; Li et al., 2002; Nielsen et al., 2007; Yu et al., 2007; Francis et al., 2011). Thus, we next wished to examine the behavior of a membrane protein that cannot participate in such interactions.

Toward this end, we transfected MDCK-S cells with a cDNA encoding a GPI-anchored protein, placental alkaline phosphatase (PLAP), and examined its distribution over time. 3 d after transfection, old PLAP was labeled by incubating live cells at 4°C with anti-PLAP antibody concurrent with BG549 labeling of old SNAP-gp135. In contrast to gp135, old PLAP did not move away from the cilium during the observation period (Fig. S2, C and D). GPI-anchored proteins, including PLAP, do not fully span the membrane bilayer and are thus unable to interact directly with cytoplasmic proteins. Therefore, we hypothesized that interactions with components of the cytoskeleton might be involved in the directed migration of gp135 away from the periciliary zone.

We used cytoskeleton-disrupting drugs to test this hypothesis. In cells treated with latrunculin A to disrupt the actin cytoskeleton (Fig. S3, A and C), delivery of gp135 to the apical membrane was decreased and new gp135 was never detected in concentrated rings at the base of the cilium (Fig. 3, A and B). Presumably because of this dramatic reduction in surface delivery of gp135, there was notably less old gp135 at the apical membrane in latrunculin A–treated cells. Interestingly, however, latrunculin A treatment did not abolish the radial movement of this remaining pool of old gp135 toward the tight junctions (Fig. S3, G and H).

After treatment with nocodazole to depolymerize microtubules (Fig. S3, B and D), old gp135 no longer moved toward the apical membrane periphery (Fig. 3, C and D; and Video 3). New BG488-labeled gp135 was observed in nocodazole-treated cells, but periciliary rings were not present (Fig. S3, I and J), although the cilia remained intact (Fig. S3, E and F). This is consistent with a previously observed 25–50% decrease in delivery of newly synthesized gp135 after nocodazole treatment (Grindstaff et al., 1998) and suggests that in addition to the latrunculin-sensitive actin cytoskeleton, microtubules play an important role in the delivery of newly synthesized gp135. The nocodazole-induced reduction of SNAP-gp135 delivery to the periciliary region does not explain nocodazole's effects on central clearing because specifically blocking delivery of newly synthesized protein with CHX did not affect central clearing (Fig. 2 B). One potential explanation for central clearing could involve selective endocytosis of apical SNAP-gp135 from the periciliary region of the apical membrane. However, microtubule depolymerization did not inhibit internalization of old gp135, as shown by the accumulation of subapical BG549-positive endosome-like structures in both untreated (Fig. S1 D) and nocodazole-treated (Fig. S3 K) samples. Thus, although we cannot rule out the possibility that nocodazole changes the localization of endocytic events, we consider this to be an unlikely explanation for the observed nocodazole sensitivity of apical spreading. Recent studies reveal the existence of a planar subapical network of microtubules that associate laterally with tight junctions (Yano et al., 2013). We believe that it is likely, therefore, that motor-driven, directed movement of gp135 along these subapical microtubules toward the tight junctions accounts for the radial central clearing.

A previous study suggested that a subset of apical proteins in MDCK cells may be delivered first to the basolateral membrane before being transcytosed to the apical surface (Polishchuk et al., 2004), although direct apical targeting of the same proteins has also been reported (Paladino et al., 2006). We took advantage of our SNAP tag system to examine whether some or all of newly delivered gp135 passes through the basolateral membrane en route to the apical surface. Surface gp135 was blocked with SBG-Block and then cells were moved to 37°C for 0–30 min, during which time a biotin-conjugated BG reagent (BG-PEG12-biotin) was present exclusively in the medium bathing the basolateral membrane to label new gp135 inserted into the basolateral plasma membrane. Streptavidin-488 was then used to visualize any biotin-labeled protein that had been transcytosed and was exposed at the apical membrane. Streptavidin-488–labeled gp135 was observed at the periciliary ring at ∼6–10 min after shifting cells to 37°C and was detected throughout the apical membrane at 30 min (Fig. 4, A and B). These data are consistent with a subset of newly synthesized gp135 traversing the basolateral membrane before apical delivery. Quantification of basolaterally labeled gp135 present at the apical membrane (Fig. 4 C, bottom left) versus the total pool of newly delivered gp135 at the apical membrane (Fig. 4 C, bottom right) demonstrated that 49.4% ± 1.5% of SNAP-gp135 pursued the transcytotic route (Fig. 4, C and D). Given that we and others (Yu et al., 2007) do not detect gp135 at the basolateral membrane in significant quantities at steady state, our data suggest that the residency time of SNAP-gp135 at the basolateral membrane is brief.

Conclusion

In summary, our results indicate a novel and surprising route for the delivery of a newly synthesized cohort of a protein to the apical membrane (Fig. 5). Microtubules and the actin cytoskeleton both participate in delivering newly synthesized gp135 to the periciliary region of the apical membrane. Interestingly, microtubules further mediate radially directed movement of cell surface gp135 away from the cilium toward the tight junctions. Our data and those of others (Thuenauer et al., 2014) indicate that this delivery behavior and radial motion is not seen with all apical membrane proteins, suggesting that multiple trafficking pathways direct targeting to and mobility within the apical membrane. According to our current working model, newly synthesized gp135 is delivered to the periciliary ring outside the septin diffusion barrier that separates the ciliary and somatic apical membranes (Hu et al., 2010). Our data demonstrate that the periciliary ring is a hot spot for the delivery of the apical protein gp135 and reveal the existence of a new epithelial trafficking pathway. These findings provide novel insights into polarized trafficking and suggest that many distinct sites of insertion are used by different apical proteins and that the post-insertion fate of an apical membrane protein is determined by exciting new processes.

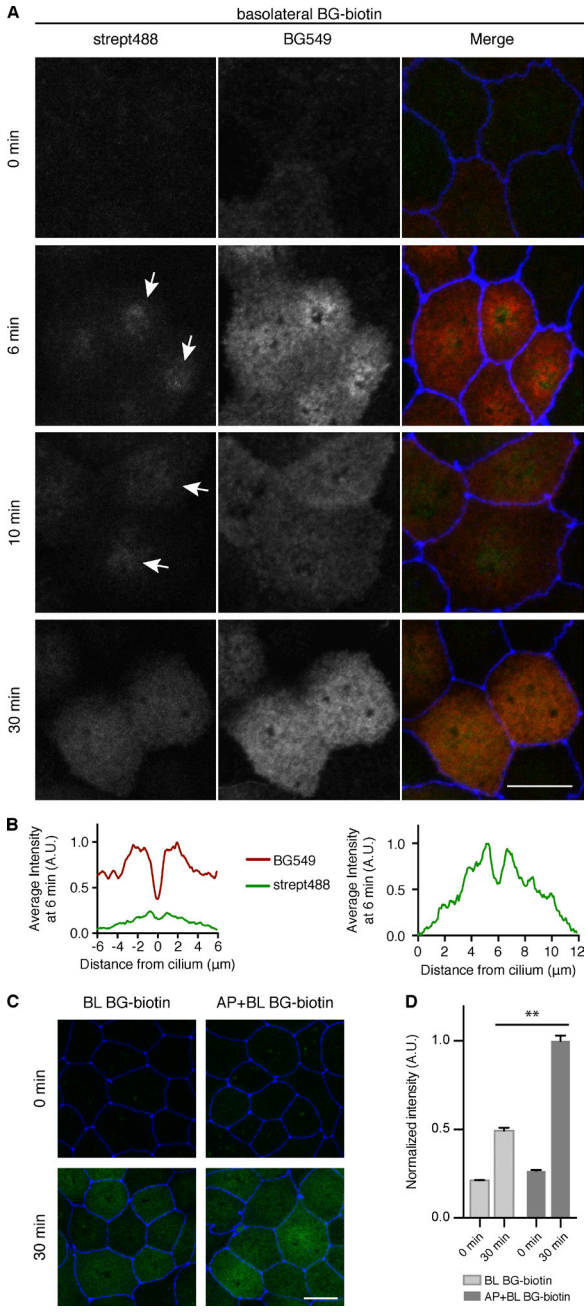

Figure 4. **A subset of gp135 is delivered to the basolateral membrane before transcytosis and delivery to the apical surface.** (A) MDCK-S cells were incubated with apical SBG-Block to block apical surface gp135. BG-PEG12-biotin was added to the medium bathing the basolateral membranes of MDCK-S cells. After a 1-h incubation at 4°C, cells were washed and moved to 37°C for 0–30 min. Cells were washed again, stained with BG549 (red) at 4°C, and then fixed for immunofluorescence with ZO1 (blue) and stained with streptavidin-488 (green). Labeling in the red channel of the merged image corresponds to gp135 that was newly delivered directly to the apical membrane. Labeling in the green channel corresponds to gp135 that was inserted first into the basolateral membrane and then delivered subsequently to the apical surface. Arrows indicate periciliary rings of transcytosed protein labeled with streptavidin-488. (B) Mean line scan intensity of streptavidin488-labeled and BG549-labeled gp135 at 6 min, as in Fig. 2 B, demonstrates delivery of transcytotic streptavidin488-labeled gp135 to the periciliary ring. All values were normalized to highest mean value of BG549 intensity at 6 min (left) or to the highest mean value of streptavidin488 intensity (right). *n* = 12 cells/condition from two independent experiments. (C and D) Surface SNAP-gp135 was blocked with SBG-Block. After washing, BG-PEG12-biotin was added to the medium, bathing either the basolateral (BL) membrane only or the apical and basolateral (AP + BL) membranes. Cells were moved to 37°C for 0 or 30 min, washed, then fixed for immunofluorescence with ZO1 (blue) and stained with streptavidin-488 (green). (C) Representative maximum-intensity projections demonstrate relative quantities of transcytosed versus total newly delivered SNAP-gp135. (D) Quantification of C normalized to streptavidin-488 intensity at 30 min in cells treated with AP + BL BG-PEG12-biotin. Values represent mean ± SEM from 186 (0 min BL), 191 (30 min BL), 161 (0 min AP + BL), and 204 (30 min AP + BL) cells. **, $P < 0.0001$. Data are representative of four independent experiments. Bars, 10 µm.

Materials and methods

Constructs and cell lines

An oligonucleotide containing the signal sequence of human gp135/podocalyxin (BC112035), the sequence for the $SNAP_f$ tag (from $pSNAP_f$; New England Biolabs), and an HA epitope tag was synthesized and inserted into pUC57 vector (GenScript). The sequence was excised using flanking EcoRI and BamHI restriction sites and inserted into pcDNA3.1(–) vector (Invitrogen). The remaining sequence for human gp135 was amplified by PCR from human cDNA (Open Biosystems) incorporating unique restriction sites and inserted at a position distal to the HA epitope tag. MDCK type II cells were stably transfected with $SNAP_f$-HA–gp135 using the Amaxa nucleofection kit T (Lonza) to create MDCK-S cells. Clones were selected and maintained in media containing 1 mg/ml G418. MDCK cells expressing SNAP-tagged Crumbs3a have been characterized elsewhere (Harder et al., 2012) and were provided by B. Margolis (University of Michigan, Ann Arbor, MI). In brief, the SNAP tag sequence was PCR amplified from the pSNAP(m) vector (New England Biolabs) and subcloned upstream of the Crumbs3a sequence in pcDNA3.1/Zeo(+). SNAP-Crumbs3a was then amplified and subcloned into pRev-TRE. Retroviral-mediated gene transfer was used to create MDCK type II cells stably expressing SNAP-Crumbs3a. Clones were selected in growth media containing 100 ng/ml hygromycin B. MDCK cells were cultured as described elsewhere (Stoops et al., 2014). Except where noted otherwise, all experiments were performed on polarized cells grown for 4–5 d on Transwell polycarbonate filters (Corning).

Apical surface delivery assay

Live MDCK-S cells or MDCK cells expressing SNAP-Crumbs3a were labeled with BG549 (1 µM), washed and treated with SNAP-Block (8 µM) in CO_2-independent media at 4°C for 30 min. Cells were washed and moved to 37°C for intervals of 0–30 min. After various intervals of incubation at 37°C, cells were returned to 4°C and surface SNAP-tagged protein was labeled with SNAP-Surface Alexa Fluor 488 (BG488, 2 µM; for confocal analysis) or SNAP-Surface 782 (SNAP782, 1 µM; for LI-COR analysis). BG reagents were obtained from New England Biolabs or provided by I. Correa (New England Biolabs Research Division, Ipswich, MA).

Where indicated, cells were pretreated with 250 µg/ml cycloheximide for 1 h at 37°C, 5 µM nocodazole for 1 h at 4°C, or 10 µM latrunculin A for 15 min at 37°C. Untreated cells were incubated with DMSO as a vehicle control. To block the recycling pool of gp135, MDCK-S cells were treated with BG549 (1 µM) for 2 h at 37°C in place of the shorter BG549 label at 4°C. To detect old PLAP at the cell surface in conjunction with an assay to detect old gp135, surface PLAP was labeled with an antibody (mouse; 1:100; Chemicon) directed against the protein's extracellular region during the 30-min BG549 4°C labeling step.

Immunofluorescence was performed as described in detail elsewhere (Stoops et al., 2014). In brief, cells were fixed in 4% paraformal-

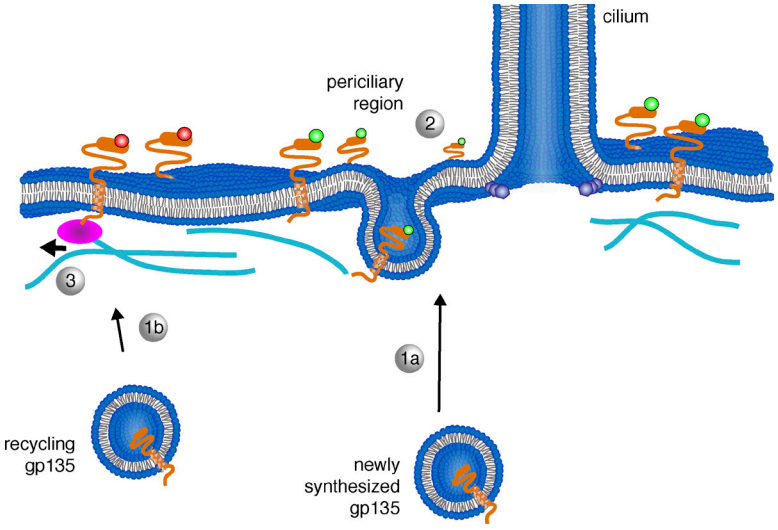

Figure 5. **Model for gp135 delivery.** Newly synthesized gp135 (1a) is delivered to the periciliary ring (2) outside the septin diffusion barrier (represented as purple beads). Recycling gp135 (1b) is delivered throughout the apical membrane. After delivery, surface gp135 demonstrates microtubule-dependent movement toward the periphery of the apical membrane (3).

dehyde and permeabilized in 0.2% saponin before sequential labeling with primary and secondary antibodies. The following primary antibodies were used: anti–ZO-1, rabbit (Invitrogen); anti–acetylated tubulin, mouse (Santa Cruz); anti–α-tubulin, mouse (Santa Cruz); and anti-ARL13B, rabbit (Abcam). Alexa Fluor (Molecular Probes) secondary antibodies were used as indicated.

Confocal microscopy

Except where specifically noted otherwise, all images were acquired on an inverted LSM 780 confocal (Carl Zeiss) microscope using a Plan-Apochromat 63×/1.40 Oil DIC M27 objective (n = 1.5 at 25°C) at room temperature. Images are the product of fourfold line averaging, with contrast and brightness settings chosen to keep all pixels in the linear range. The LSM 780 is equipped with two cooled photomultiplier tubes and a 32-channel array of Gallium Arsenide Phosphide detectors. Images were captured using ZEN software (Carl Zeiss) and processed using ImageJ (National Institutes of Health) and Volocity (PerkinElmer) software. The plot profile function in ImageJ was used to quantify gp135 intensity across the apical membrane, with the ciliary exclusion zone centered at point 0. Line intensity data were normalized to the highest and lowest mean values within each channel for each treatment condition, except where noted otherwise.

Western blot analysis

After labeling of newly delivered SNAP-gp135 with SNAP782, cells were lysed in TNT buffer (50 mM Tris-HCl, pH 7.5, 100 mM NaCl, 1% Triton X-100, 1 mM DTT, and complete EDTA-free protease inhibitors [Roche]). Lysates were subjected to SDS-PAGE, Western blot, and LI-COR analysis, as described in detail elsewhere (Stoops et al., 2014). Primary antibodies used included anti-HA (mouse; Covance) and anti–β-actin as a loading control (mouse; Abcam). Quantification was performed using LI-COR Odyssey software.

Live imaging

MDCK-S cells were grown in MatTek dishes for 2 d. Where noted, cells were preincubated with 0.8 µM SNAP-Block for 30 min at 4°C, followed by removal of SNAP-Block and recovery for the indicated amount of time at 37°C. Surface protein was labeled for 1 min with 2 µM BG488 at 37°C and cells were then washed. Cells were visualized on a Yokagawa-type spinning disc confocal microscope system controlled by Volocity software (PerkinElmer). The system was mounted onto an inverted microscope (IX-71; Olympus) equipped with a 1 × 1-Kb electron-multiplying charge-coupled device camera (Hamamatsu Photonics) and a temperature-controlled stage set at 37°C. Cells were imaged using a 60× oil 1.4 NA oil phase objective.

Statistics

Prism software, version 6.0 (GraphPad), was used for all statistical analysis, including calculation of basic statistical values (mean and SEM). Statistical significance was determined using an unpaired Student's t test (two-tailed, with the exception of Fig. 2 D, which was one-tailed). The ROUT method (Q = 0.1%) was used to remove one outlier from six replicates in the 0-min steady-state time point in Fig. 2 D. No other values were excluded.

MATLAB (MathWorks) was used to determine the quantity of SNAP-gp135 that pursues the transcytotic route. Briefly, maximum-intensity projections were generated and the ZO1 signal was used to outline cells and to thus generate a mask for cell-specific quantification. Per-cell intensity values for BG549 (SNAP-gp135) were calculated in MATLAB for cells labeled basolaterally versus BG549 staining in cells labeled both basolaterally and apically. The resulting data were analyzed using Prism software.

Online supplemental material

Fig. S1 shows Western blot analysis of MDCK-S cells and internalization of surface gp135 into endocytic compartments. Fig. S2 shows that Crumbs3a is delivered to the apical membrane and tight junctions and that the GPI-anchored surface protein PLAP is not cleared from the periciliary region over time. Fig. S3 shows the effects of latrunculin A and nocodazole treatment on F-actin and microtubules, respectively, as well as additional data on each drug's effect on cilia and gp135 trafficking. Video 1 shows delivery of SNAP-gp135 to the periciliary ring in live MDCK-S cells. Video 2 shows time-lapse imaging of the central clearing of old SNAP-gp135 over time in MDCK-S cells. Video 3 shows inhibition of SNAP-gp135 central clearing in nocodazole-treated MDCK-S cells. Online supplemental material is available at http://www.jcb.org/cgi/content/full/jcb.201502045/DC1.

Acknowledgments

This manuscript is dedicated with love and respect to the memory of Michael Hull, who made critically important contributions to this work and whose intellect, ability, humor, and friendship are very deeply missed.

The authors would like to thank Vanathy Rajendran for generation of the PLAP construct; Drs. Pietro De Camilli, Christa Cortesio, and David

Drubin for critical reading of the manuscript; Dr. Benjamin Margolis and Dr. Ivan Correa for their helpful advice and gifts of important reagents; and all of the members of the Caplan laboratory for helpful discussions and support.

This work was supported by National Institutes of Health (NIH) training grant 5T32GM007223-35 and National Science Foundation Graduate Research Fellowship grant no. DGE-1122492 (E.H. Stoops) and NIH grants DK17433 and DK072612 (M.J. Caplan).

The authors declare no competing financial interests.

Submitted: 12 February 2015
Accepted: 18 September 2015

References

Cao, X., U. Coskun, M. Rössle, S.B. Buschhorn, M. Grzybek, T.R. Dafforn, M. Lenoir, M. Overduin, and K. Simons. 2009. Golgi protein FAPP2 tubulates membranes. *Proc. Natl. Acad. Sci. USA.* 106:21121–21125. http://dx.doi.org/10.1073/pnas.0911789106

Doyonnas, R., D.B. Kershaw, C. Duhme, H. Merkens, S. Chelliah, T. Graf, and K.M. McNagny. 2001. Anuria, omphalocele, and perinatal lethality in mice lacking the CD34-related protein podocalyxin. *J. Exp. Med.* 194:13–27. http://dx.doi.org/10.1084/jem.194.1.13

Ellis, M.A., B.A. Potter, K.O. Cresawn, and O.A. Weisz. 2006. Polarized biosynthetic traffic in renal epithelial cells: Sorting, sorting, everywhere. *Am. J. Physiol. Renal Physiol.* 291:F707–F713. http://dx.doi.org/10.1152/ajprenal.00161.2006

Farr, G.A., M. Hull, I. Mellman, and M.J. Caplan. 2009. Membrane proteins follow multiple pathways to the basolateral cell surface in polarized epithelial cells. *J. Cell Biol.* 186:269–282. http://dx.doi.org/10.1083/jcb.200901021

Francis, S.S., J. Sfakianos, B. Lo, and I. Mellman. 2011. A hierarchy of signals regulates entry of membrane proteins into the ciliary membrane domain in epithelial cells. *J. Cell Biol.* 193:219–233. http://dx.doi.org/10.1083/jcb.201009001

Grindstaff, K.K., R.L. Bacallao, and W.J. Nelson. 1998. Apiconuclear organization of microtubules does not specify protein delivery from the trans-Golgi network to different membrane domains in polarized epithelial cells. *Mol. Biol. Cell.* 9:685–699. http://dx.doi.org/10.1091/mbc.9.3.685

Harder, J.L., E.L. Whiteman, J.N. Pieczynski, C.-J. Liu, and B. Margolis. 2012. Snail destabilizes cell surface Crumbs3a. *Traffic.* 13:1170–1185. http://dx.doi.org/10.1111/j.1600-0854.2012.01376.x

Hu, Q., L. Milenkovic, H. Jin, M.P. Scott, M.V. Nachury, E.T. Spiliotis, and W.J. Nelson. 2010. A septin diffusion barrier at the base of the primary cilium maintains ciliary membrane protein distribution. *Science.* 329:436–439. http://dx.doi.org/10.1126/science.1191054

Juillerat, A., T. Gronemeyer, A. Keppler, S. Gendreizig, H. Pick, H. Vogel, and K. Johnsson. 2003. Directed evolution of O6-alkylguanine-DNA alkyltransferase for efficient labeling of fusion proteins with small molecules in vivo. *Chem. Biol.* 10:313–317. http://dx.doi.org/10.1016/S1074-5521(03)00068-1

Keppler, A., M. Kindermann, S. Gendreizig, H. Pick, H. Vogel, and K. Johnsson. 2004. Labeling of fusion proteins of O6-alkylguanine-DNA alkyltransferase with small molecules in vivo and in vitro. *Methods.* 32:437–444. http://dx.doi.org/10.1016/j.ymeth.2003.10.007

Kerjaschki, D., D.J. Sharkey, and M.G. Farquhar. 1984. Identification and characterization of podocalyxin--the major sialoprotein of the renal glomerular epithelial cell. *J. Cell Biol.* 98:1591–1596. http://dx.doi.org/10.1083/jcb.98.4.1591

Kreitzer, G., J. Schmoranzer, S.H. Low, X. Li, Y. Gan, T. Weimbs, S.M. Simon, and E. Rodriguez-Boulan. 2003. Three-dimensional analysis of post-Golgi carrier exocytosis in epithelial cells. *Nat. Cell Biol.* 5:126–136. http://dx.doi.org/10.1038/ncb917

Li, Y., J. Li, S.W. Straight, and D.B. Kershaw. 2002. PDZ domain-mediated interaction of rabbit podocalyxin and Na(+)/H(+) exchange regulatory factor-2. *Am. J. Physiol. Renal Physiol.* 282:F1129–F1139. http://dx.doi.org/10.1152/ajprenal.00131.2001

Louvard, D. 1980. Apical membrane aminopeptidase appears at site of cell-cell contact in cultured kidney epithelial cells. *Proc. Natl. Acad. Sci. USA.* 77:4132–4136. http://dx.doi.org/10.1073/pnas.77.7.4132

Lukinavičius, G., K. Umezawa, N. Olivier, A. Honigmann, G. Yang, T. Plass, V. Mueller, L. Reymond, I.R. Corrêa Jr., Z.-G. Luo, et al. 2013. A near-infrared fluorophore for live-cell super-resolution microscopy of cellular proteins. *Nat. Chem.* 5:132–139. http://dx.doi.org/10.1038/nchem.1546

Makarova, O., M.H. Roh, C.-J. Liu, S. Laurinec, and B. Margolis. 2003. Mammalian Crumbs3 is a small transmembrane protein linked to protein associated with Lin-7 (Pals1). *Gene.* 302:21–29. http://dx.doi.org/10.1016/S0378111902010843

Maurel, D., S. Banala, T. Laroche, and K. Johnsson. 2010. Photoactivatable and photoconvertible fluorescent probes for protein labeling. *ACS Chem. Biol.* 5:507–516. http://dx.doi.org/10.1021/cb1000229

Meder, D., A. Shevchenko, K. Simons, and J. Füllekrug. 2005. Gp135/podocalyxin and NHERF-2 participate in the formation of a preapical domain during polarization of MDCK cells. *J. Cell Biol.* 168:303–313. http://dx.doi.org/10.1083/jcb.200407072

Nielsen, J.S., M.L. Graves, S. Chelliah, A.W. Vogl, C.D. Roskelley, and K.M. McNagny. 2007. The CD34-related molecule podocalyxin is a potent inducer of microvillus formation. *PLoS One.* 2:e237. http://dx.doi.org/10.1371/journal.pone.0000237

Ojakian, G.K., and R. Schwimmer. 1988. The polarized distribution of an apical cell surface glycoprotein is maintained by interactions with the cytoskeleton of Madin-Darby canine kidney cells. *J. Cell Biol.* 107:2377–2387. http://dx.doi.org/10.1083/jcb.107.6.2377

Paladino, S., T. Pocard, M.A. Catino, and C. Zurzolo. 2006. GPI-anchored proteins are directly targeted to the apical surface in fully polarized MDCK cells. *J. Cell Biol.* 172:1023–1034. http://dx.doi.org/10.1083/jcb.200507116

Polishchuk, R., A. Di Pentima, and J. Lippincott-Schwartz. 2004. Delivery of raft-associated, GPI-anchored proteins to the apical surface of polarized MDCK cells by a transcytotic pathway. *Nat. Cell Biol.* 6:297–307. http://dx.doi.org/10.1038/ncb1109

Stoops, E.H., and M.J. Caplan. 2014. Trafficking to the apical and basolateral membranes in polarized epithelial cells. *J. Am. Soc. Nephrol.* 25:1375–1386. http://dx.doi.org/10.1681/ASN.2013080883

Stoops, E.H., G.A. Farr, M. Hull, and M.J. Caplan. 2014. SNAP-tag to monitor trafficking of membrane proteins in polarized epithelial cells. *Methods Mol. Biol.* 1174:171–182. http://dx.doi.org/10.1007/978-1-4939-0944-5_11

Sun, X., A. Zhang, B. Baker, L. Sun, A. Howard, J. Buswell, D. Maurel, A. Masharina, K. Johnsson, C.J. Noren, et al. 2011. Development of SNAP-tag fluorogenic probes for wash-free fluorescence imaging. *ChemBioChem.* 12:2217–2226. http://dx.doi.org/10.1002/cbic.201100173

Thuenauer, R., Y.-C. Hsu, J.M. Carvajal-Gonzalez, S. Deborde, J.-Z. Chuang, W. Römer, A. Sonnleitner, E. Rodriguez-Boulan, and C.-H. Sung. 2014. Four-dimensional live imaging of apical biosynthetic trafficking reveals a post-Golgi sorting role of apical endosomal intermediates. *Proc. Natl. Acad. Sci. USA.* 111:4127–4132. http://dx.doi.org/10.1073/pnas.1304168111

Vieira, O.V., K. Gaus, P. Verkade, J. Fullekrug, W.L.C. Vaz, and K. Simons. 2006. FAPP2, cilium formation, and compartmentalization of the apical membrane in polarized Madin-Darby canine kidney (MDCK) cells. *Proc. Natl. Acad. Sci. USA.* 103:18556–18561. http://dx.doi.org/10.1073/pnas.0608291103

Yano, T., T. Matsui, A. Tamura, M. Uji, and S. Tsukita. 2013. The association of microtubules with tight junctions is promoted by cingulin phosphorylation by AMPK. *J. Cell Biol.* 203:605–614. http://dx.doi.org/10.1083/jcb.201304194

Yu, C.-Y., J.-Y. Chen, Y.-Y. Lin, K.-F. Shen, W.-L. Lin, C.-L. Chien, M.B.A. ter Beest, and T.-S. Jou. 2007. A bipartite signal regulates the faithful delivery of apical domain marker podocalyxin/Gp135. *Mol. Biol. Cell.* 18:1710–1722. http://dx.doi.org/10.1091/mbc.E06-07-0629